JOC The Journal of Organic Chemistry

Article

pubs.acs.org/joc

Stacked Naphthyls and Weak Hydrogen-Bond Interactions Govern the Conformational Behavior of *P*-Resolved Cyclic Phosphonamides: A Combined Experimental and Computational Study

Maria Annunziata M. Capozzi,[†] Francesco Capitelli,[‡] Andrea Bottoni,[§] Matteo Calvaresi,[§] and Cosimo Cardellicchio*[,∥]

[†]Dipartimento di Chimica, Università di Bari, via Orabona 4, Bari, Italy

[‡]CNR IC, via Salaria, Km 29.300, Monterotondo (Rome), Italy

[§]Dipartimento di Chimica G. Ciamician, Università di Bologna, via Selmi 2, Bologna, Italy

[∥]CNR ICCOM, Dipartimento di Chimica, Università di Bari, via Orabona 4, 70125 Bari, Italy

Supporting Information

ABSTRACT: *P*-Enantiomerically pure cyclic phosphonamides have been synthesized via a cyclization reaction of (*S*,*S*)-aminobenzylnaphthols with chloromethylphosphonic dichloride. The reaction is highly stereoselective and gives almost exclusively (*S*,*S*,S_P)-cyclic phosphonamides in good yields. Analysis of the X-ray crystal structures shows clearly that the cyclization reaction forces the two naphthyl rings into a stable parallel displaced stacking assembly and indicates also the existence of intramolecular CH···π interactions and weak forms of intermolecular hydrogen bondings, involving the oxygen and the chlorine atoms. QM computations and NMR spectra in solution confirm the stacked molecular assembly as the preferred arrangement of the two naphthyl groups.

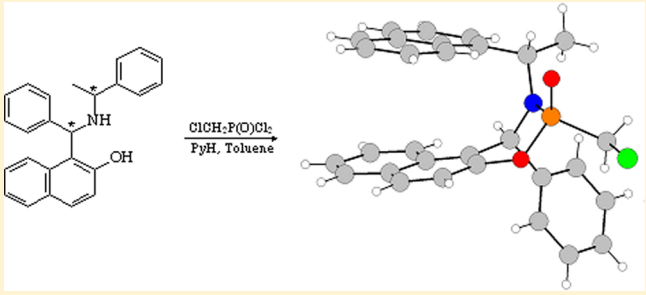

INTRODUCTION

Organic derivatives of phosphonic acid have been commonly employed in organic synthesis.[1−3] The practical utility of these compounds can be ascribed to the capacity of the phosphonyl moiety to stabilize carbanions and to the degree of asymmetric induction produced by the phosphorus stereogenic center.[1−3]

Moreover, since the phosphonyl group represents an isostere of the carbonyl group, many applications of these molecules to medicinal chemistry have been described in the literature.[4] One interesting example is provided by α-aminophosphonic acids: these phosphonic compounds are the isosteric analogues of α-amino acids and can influence a considerable number of physiologic and pathologic processes by inhibiting some specific enzymes.[5,6]

A particularly interesting class of phosphorus bioactive molecules is represented by the cyclic phosphonamides, which are six-membered rings characterized by the N−P(O)−O scaffold. Some of them were reported to be active against various disease states, such as the hepatitis B virus.[7] The most representative member of this class is "cyclophosphamide", one of the best known anticancer chemotherapeutic agents.[8] Its mechanism of action is related to the in vivo production of a powerful anticancer nitrogen mustard. Thanks to its proven biological activity, "cyclophosphamide" is linked to a long list of structurally similar prodrugs[8,9] and has inspired many investigations[8] into its mechanism of action.

It is worth noting that, in addition to "cyclophosphamide", other cyclic phosphonamides exhibit a marked anticancer action. This action is related to the ability of these compounds to inhibit matrix metalloproteinase (MMP). It is known that the uncontrolled expression and activity of MMPs is responsible for a number of diseases, among them tumor growth and metastasis.[10] In particular, cyclic aryl phosphonamides have been shown to have increased citoxicity because the electron-poor aryl ring favors the prodrug cleavage and the formation of an active mustard.[11]

Considering the interest shown in these compounds as bioactive molecules, therapeutic agents, and their potential synthetic applications, the present work examines the possibility for synthesis of new *P*-chiral cyclic phosphonamides.

The synthesis of *P*-chiral intermediates[12] is generally associated with a multistep process. First, diastereomeric phosphorus intermediates must be prepared with the aid of a chiral auxiliary, and then the separation of the resulting epimers with different chirality at the phosphorus center must be carried out. Finally, stereocontrolled reaction steps complete the synthetic procedure leading to the target *P*-resolved product. In previous work on this topic, natural menthol was used as a

Received: September 10, 2014
Published: October 23, 2014

dx.doi.org/10.1021/jo502094g | J. Org. Chem. 2014, 79, 11101−11109

chiral auxiliary to synthesize *P*-chiral phospine oxides[13] or sulfinylmethylphosphonates.[14]

In the course of our research on asymmetric synthesis, the Betti reaction was rediscovered.[15,16] Since then, this procedure has been applied by others[17] for the synthesis of new aminobenzylnaphthols that were employed as chiral auxiliaries.

Using the Betti procedure for the synthesis of (*S*,*S*)-aminobenzylnaphthols,[18] it was decided to investigate the possibility of producing cyclic phosphonamides, with formation of a novel stereogenic center at the phosphorus atom, by reacting these aminobenzylnaphthols with a phosphonic dichloride. Herein, we report the results of this ring-closing reaction, which demonstrated an unexpected high stereoselection toward the (*S*,*S*,S_P)-epimers. The synthetic work was accompanied by a structural analysis of the crystals of these compounds and by a detailed conformational study based on density functional theory (DFT) computations.

RESULTS AND DISCUSSION

1. Chiral Auxiliaries via Betti Reaction: Synthesis of Aminobenzylnaphthols. Aminobenzylnaphthols **1a**−**4a**[18] were obtained after reaction of 2-naphthol, (*S*)-1-naphthylethylamine, and benzaldehyde (**1a**) or 4-halobenzaldehyde (**2a**−**4a**) as shown in Scheme 1.

Scheme 1. Betti Reaction (X = H (1a); X = F (2a); X = Cl (3a); X = Br (4a))

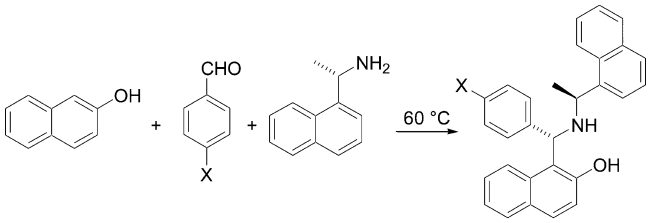

X= H, F, Cl, Br **1a-4a**

This multicomponent but straightforward condensation, performed without solvent, led exclusively to formation of the (*S*,*S*)-aminobenzylnaphthols in satisfactory isolated yields (51−68%). Only a simple crystallization of the crude reaction mixture was carried out.[18] Convergence of the Betti reaction toward the (*S*,*S*)- or (*R*,*R*)-stereoisomers was explained by Palmieri et al. by invoking the preferential crystallization of these diastereoisomers in the reaction mixture.[19] Investigation of the crystal structures of (*S*,*S*)-aminobenzylnaphthol highlighted many short-distance interactions involving the aryl groups.[18] These interactions can be reasonably assumed to be one of the key factors that contribute to the crystal stability of the (*S*,*S*)-stereoisomers and thus to high stereoselection of the Betti reaction toward these stereoisomers.[18]

2. Synthesis of (*S*,*S*,S_P)-Cyclic Phosphonamides. Cyclic phosphonamides **1b**−**4b** were obtained via the ring-closing reaction of (*S*,*S*)-aminobenzylnaphthols **1a**−**4a** with chloromethylphosphonic dichloride (Scheme 2). This phosphonic dichloride was selected as the electrophilic reactant just like the procedure described in the work carried out by Sisti et al.,[20] Hanessian et al.,[21,22] and Lopez et al.[23] in which potential precursors of antiviral agents were prepared.

After a preliminary screening of the reaction conditions, cyclized products were obtained using toluene as a reaction solvent in the presence of pyridine (Scheme 2). Under these

Scheme 2. Ring-Closing Reaction of Aminobenzylnaphthols 1a−4a Using Chloromethylphosphonic Dichloride

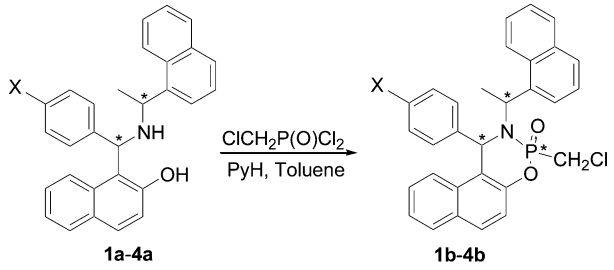

1a-4a **1b-4b**

X=H, F, Cl, Br

conditions, the reaction led to good isolated yields (73−91%, see the Experimental Section) of the valuable (*S*,*S*,*S*p)-cyclic phosphonamides **1b**−**3b**. The only exception was the reaction affording cyclic phosphonamide **4b** (50% yield). No trace of the (*S*,*S*,*R*p)-epimers of cyclic phosphonamides **1b**−**2b** was detected for the reaction starting from **1a**−**2a**. Small amounts (<5%) of side products having NMR spectra compatible with the structure of the (*S*,*S*,*R*p)-epimers of cyclic phosphonamides **3b**−**4b** were observed, and they were easily separated from the main reaction product. Investigations associated with these products were not carried out at this time, even if some considerations about them are developed later.

In conclusion, with the use of the ring-closing reaction described above, the difficult task was achieved of obtaining in a single step and in good yields cyclic phosphonamides with three resolved stereogenic centers including the just formed *P*-stereogenic center. This result was obtained in the absence (or with negligible levels) of different *P*-epimers.

As a result of the high stereoselection of the cyclization reaction toward the (*S*,*S*,*S*p)-cyclic phosphonamides, we decided to investigate the crystal structures of the synthesized intermediates **1b**−**4b** to identify specific interactions (solid phase) that might be responsible for the observed stereochemical outcome.

3. Crystal Structures of (*S*,*S*,S_P)-Cyclic Phosphonamides: Intra- and Intermolecular Interactions. We found that crystals of cyclic phosphonamides **1b**−**4b** were suitable for X-ray diffraction analysis and could establish the configuration of these stereocenters in the cyclic phosphonamide products a (*S*,*S*,S_P). The crystal structures of **1b**, **3b**, and **4b** are orthorhombic (space group is $P2_12_12_1$), and a single molecule is hosted in the asymmetric unity. Two molecules are hosted in the asymmetric unit in the case of **2b** (see Table S1 and Figures S1−S4 of the Supporting Information).

In all species, the six-membered ring including oxygen, phosphorus, and nitrogen atoms (C−C−C−O−P−N) dictates the central features of the entire structure. The two sp2 carbon atoms are shared with the adjacent naphthyl group and the oxygen lies approximately in the plane of the three carbon atoms of the cycle: the measured dihedral angles between the plane of these carbon atoms and the reference plane of the oxygen atom (angle between the two planes C−C−C and C−C−O) are in the range 3°−5° in all cases (**1b**−**4b**). The phosphorus and nitrogen atoms force the ring into a twist-boat conformation, which is reported elsewhere for related cyclic phosphonamides.[24,25] These structural features are evident in the prototype cyclic phosphonamide **1b** depicted in Figure 1 as a representative example.

dx.doi.org/10.1021/jo502094g | J. Org. Chem. 2014, 79, 11101−11109

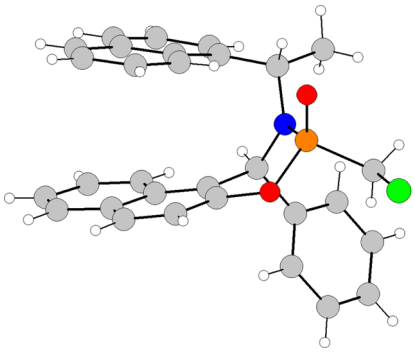

Figure 1. Crystal structures of cyclic phosphonamides **1b**.

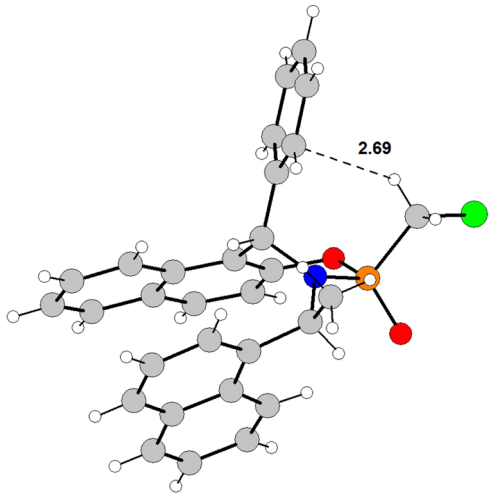

Figure 2. Intramolecular CH···π interactions in cyclic phosphonamides **1b**.

The (S_P) configuration in the twist-boat conformation of the cyclic phosphonamide ring is characterized by axial and equatorial positions of the phosphonic oxygen and chloromethyl group, respectively (Figure 1).

It is apparent that the twist-boat conformation of the six-member ring has a moderate conformational freedom. However, two conformational motifs are of particular interest in **1b**−**4b**. The first one is the rotation of the 1-naphthylethyl moiety around the bond between the nitrogen and the exocyclic carbon atom. Crystal structure analysis shows that, thanks to this conformational freedom, the two naphthyl groups preferentially form intramolecular parallel displaced stacking structure as shown, for example, in Figure 1.

Even in the crystal structures where the phenyl group and the two naphtyl groups of the starting (*S*,*S*)-aminobenzylnaphthols **1a**−**4a** are arranged *anti* one from the other,[18] the cyclization reaction with chloromethylphosphonic dichloride has the effect of forcing the naphthyl moieties into a particular stacking arrangement that promotes π-stacking interactions.

The second conformational motif is rotation of the chloromethyl group around the bond between phosphorus and the chloromethyl carbon atom. The crystal structure analysis suggests the existence of a CH···π interaction[26−28] between one hydrogen of the methylene moiety and the phenyl group. A schematic representation of this intramolecular interaction in **1b**, chosen as a representative example, is given in Figure 2, where **1b** is just represented in a different 3-D perspective with respect to Figure 1.

The nature of CH···π interactions has been thoroughly investigated,[26−28] and it has become evident that, in spite of their weakness, these interactions can play a significant role in many different fields of research.[26−28] The importance of CH···π interactions in determining the high enantioselectivity observed in the asymmetric oxidation of aryl benzyl sulfides using hydroperoxides in the presence of a titanium catalyst has recently been described.[29−31] In some recent studies, CH···π interactions were indicated as "CH···π hydrogen bondings" to denote them as the weakest form of the hydrogen bonds.[28]

As shown in Figure 2, one hydrogen atom of the methylene group of **1b**−**4b** points toward the plane of the phenyl group. The distances between the methylene hydrogen atom and the phenyl plane are in the range 2.69−2.72 Å. Geometrical parameters that characterize this interaction are reported in the Supporting Information (Table S2 and Figure S5). The values of these parameters are in agreement with the existence of a non-negligible interaction[26−28] that should restrain the rotation around the carbon−phosphorus bond and that should provide a further energetic stabilization to the structure. In fact, in the (*S*,*S*,R_P)-cyclic phosphonamides epimers, which are characterized by equatorial and axial positions of the phosphonic oxygen and chloromethyl group, respectively, the CH···π interaction involving the methylene hydrogen atoms is not present because the hydrogen atoms have no proximity with phenyl or naphthyl rings. Consequently, energetic stabilization of the structure due to CH···π interactions is missing in (*S*,*S*,R_P)-cyclic phosphonamides, and this fact might explain the stereoselection of the ring-closing reaction toward the stabilized (*S*,*S*,S_P)-stereoisomers.

The crystal structures of cyclic phosphonamides **1b**−**4b** are built up by intermolecular CH···O weak hydrogen bondings[32] involving the phosphonyl oxygen atom and one naphthyl hydrogen atom of two adjacent molecules, as shown in Figure 3. Geometrical parameters describing the most important C−H···O interactions are summarized in Table 1.

Given the common features of the crystal structures of cyclic phosphonamides **1b**−**4b**, the presence of the halogen atom in the *para*-position of the phenyl group in molecules **2b**−**4b**, resulting as a consequence of the employment of *p*-halobenzaldeydes in the Betti condensation reaction, affords further minor structural differences. The main difference is that, in compound **1b**, the chlorine atom of the chloromethyl group of one molecule and one naphthyl hydrogen atom of an adjacent molecule are involved into a CH···Cl interaction[33] (Table 1, entry 4). This interaction is another example of hydrogen bonding in which the chlorine atom behaves as an acceptor. On the other hand, in the almost isostructural cyclic phosphonamides **3b** and **4b**, the chlorine atom of the chloromethyl group interacts with the naphthyl π-system of another molecule. This interaction can be considered one form of the halogen bonding.[34]

4. Quantum Mechanical (QM) and NMR Analysis on the Main Conformers. QM conformational analysis and NMR experiments have been carried out to investigate the two above-described conformational motifs and compare the behavior of cyclic phosphonamides in solid phase and solution in which the constraints of the crystal packing disappear. In the following discussion, we use the labels reported in Figures 4 and 6 (and in Figure S7 of the Supporting Information) to denote the various atoms involved in the discussion.

dx.doi.org/10.1021/jo502094g | J. Org. Chem. 2014, 79, 11101−11109

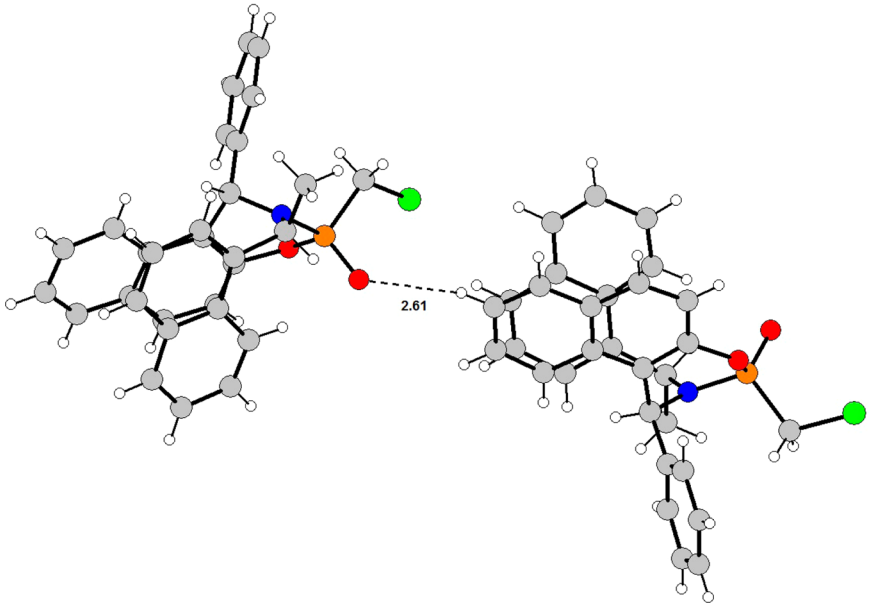

Figure 3. Intermolecular CH···O short contacts in cyclic phosphonamide **1b**.

Table 1. Distance (Å) and Angles (deg) for Intermolecular Hydrogen Bond Interactions

entry	compd	D−X···A[a]	H···A	D···A	∠D−H···A	symmetry
1	**1b**	C9−H9···O2[a]	2.61	3.499(5)	160.7	$-x + {}^{1}/_{2}, -y, +z - {}^{1}/_{2}$
2	**3b**	C6−H6···O2[b]	2.51	3.411(6)	162.2	$x + 1/2, -y + {}^{1}/_{2} + 1, -z + 1$
3	**4b**	C6−H6···O2[b]	2.56	3.459(8)	161.4	$x + {}^{1}/_{2}, -y + {}^{1}/_{2} + 1, -z + 1$
4	**1b**	C6−H6···Cl1[c]	2.95	3.627(5)	130.8	$x - {}^{1}/_{2}, -y - {}^{1}/_{2}, -z + 2$

[a]The crystallographic notation corresponds to the following interactions: (a) phosphonyl oxygen atom with hydrogen atom in position 8 of naphthyl group that is a part of cyclophosphonamide ring; (b) phosphonyl oxygen atom with hydrogen atom in position 4 of naphthyl group that is a part of cyclophosphonamide ring; (c) chlorine atom of chloromethyl group with hydrogen atom in position 4 of the naphthyl group that is a part of cyclophosphonamide ring.

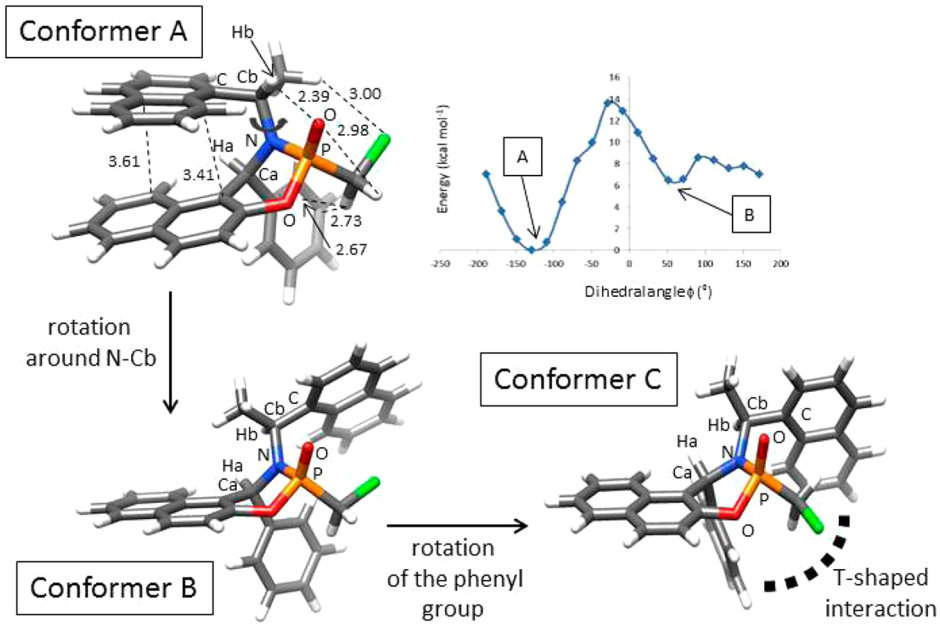

Figure 4. Conformational analysis along the dihedral angle ϕ. Schematic representation of conformers A−C. C is obtained along a different conformational coordinate describing the rotation of the phenyl group and orthogonal to ϕ. Energy values are expressed in kcal mol^{-1} and distances in angstroms.

4.1. NMR Spectra. General Aspect. The ^{1}H NMR spectra (see the Experimental Section and the Supporting Information, Figures S6−S16) show a characteristic pattern of the alkyl hydrogen atoms for each molecule **1b−4b**. The hydrogen bond

dx.doi.org/10.1021/jo502094g | J. Org. Chem. 2014, 79, 11101−11109

to the exocyclic carbon H_b is a multiplet in the range 6.20−6.11 ppm (dq when better resolved, see compound **2b**) due to the coupling of H_b with the phosphorus atom and the hydrogen atoms of the methyl group. The hydrogen bond to the endocyclic carbon H_a is a doublet in the range 5.61−5.53 ppm, due to the coupling with the phosphorus atom. The methylene hydrogen atoms is a dd, due to the geminal coupling with the other hydrogen and with the phosphorus nucleus. One of them has a chemical shift in the range 3.34−3.28 ppm. The other one moves to high field (2.69−2.61 ppm), thus producing an almost 0.7 ppm difference between these chemical shifts. This shift can be considered a clear indication that also in solution the hydrogen atom having a high field signal is facing the phenyl group[26−28] (see Figure S7 of the Supporting Information for more details).

As previously noted, the less abundant stereoisomers (S,S,R_P)-**3b** and -**4b** were obtained in such small quantities that a complete characterization was not achieved. However, the section of the ^{1}H NMR spectrum between 6.3 and 2.4 ppm was free from unrelated signals and was analyzed (see the Supporting Information, Figure S15, in which the ^{1}H NMR spectra of (S, S, S_P)-**4b** and of (S, S, R_P)-**4b** are compared). The position of the signals related to hydrogen atoms H_a and H_b is inverted, but the most interesting feature is that the methylene hydrogen atoms of (S,S,R_P)-**4b** have a similar chemical shift (3.57 and 3.34 ppm); i.e., there is no high field shift of one of them, as occurs in (S,S,S_P)-**4b**. These similar chemical shifts can be justified on the basis of the fact that the methylene group of (S,S,R_P)-**4b** is placed in an apical position, and thus, it cannot interact with the phenyl moiety, with the consequent high field shift.

4.2. Rotation of the 1-Naphthylethyl Group. We have first analyzed the rotational motion of the 1-naphthylethyl group around the bond between nitrogen and the exocyclic carbon atom C_b in the prototype molecule **1b**. This motion determines the relative orientation of the two naphthyl groups and is described by the dihedral angle ϕ defined by the two planes P−N−C_b and N−C_b−C [P−(N−C_b)−C] angle. The nature of this rotation is depicted in Figure 4, as well as the diagram (top right) that describes the optimized energy profile obtained for discrete increments of dihedral angle ϕ.

The QM computations indicate that, as found in solid phase, the most stable structure in solution is conformer A (ϕ = −128.3°), which favors the π-stacking interactions between the two naphthyl groups. These interactions are represented in Figure 4 where we have evidenced two of the shortest distances between the carbon atoms of the two naphthyl groups. Recent calculations showed that the entity of the interaction between two naphthalenes in a naphthalene dimer is 5.51 and 5.62 kcal mol^{-1} for the crossed and graphite-type dimers, respectively.[35,36] When the two naphthyl moieties in **1b** are far away and cannot interact, as found in Conformer B (minimum at ϕ = 51.7° as shown in Figure 4), the energy becomes 6.5 kcal mol^{-1} higher than conformer A, in agreement with the previously reported computed values. Partial stabilization is obtained after rotation of the phenyl ring in conformer B to afford conformer C, where a T-shaped interaction between the phenyl and one of the naphthyl groups is established. Conformer C is not represented in the diagram of Figure 4 since it exists along a different conformational coordinate describing the rotation of the phenyl group and orthogonal to ϕ. Conformer C is 1.3 kcal mol^{-1} lower than conformer B but remains 5.2 kcal mol^{-1} less stable than conformer A. On the basis of this energy difference, we obtain a population of 99.98% for the crystallographic conformer A versus a value of 0.02% for conformer C. Thus, the results of our computational investigations demonstrate that even in solution the molecule appears to be "frozen" in a conformation in which the relative arrangement of the two naphthyl groups is a parallel-displaced stacking structure, very similar to that found in the crystal structure. The solvent effects (chloroform) have been taken into account in our computations using the polarizable continuum model (PCM) approach with a dielectric constant ε of 4.71 (see the final Computational Methods for more details).

The NMR spectra were used as a further experimental validation of the computational results. In a first instance, we thought to study the rotation of the 1-naphthylethyl group by analyzing the ^{3}J coupling constants of the phosphorus nucleus with the H_b hydrogen atom (bonded to the exocyclic carbon C_b). However, the attempt to discriminate between Conformer A and Conformer B with this technique cannot be successful because, as previously reported, the dihedral angle ϕ is −128.3° and 51.7° for A and B, respectively. Since the Karplus-like behavior of this coupling constants follows a cos^2 ϕ trend,[37] it is reasonable to believe that the coupling constants will have similar values. Analogous arguments hold also for the ^{3}J constant between the phosphorus nucleus and two carbon atoms. On the other hand, the comparison between the experimental (see Experimental Section) and calculated ^{1}H NMR chemical shifts of the two hydrogen atoms H_a (bonded to the endocyclic carbon C_a) and H_b (bonded to the exocyclic carbon C_b) validates our hypothesis pointing to conformer A as the dominant structure in solution. The computed chemical shifts of H_a and H_b for conformers A are 5.57 and 6.12 ppm, respectively, which agree very well with the corresponding experimental values of 5.61 and 6.15 ppm (see also Figure 5).

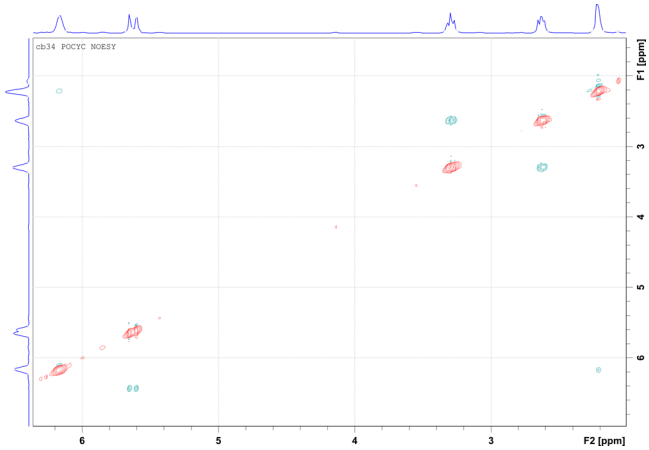

Figure 5. NOESY experiment for molecule **1b.** Only the signals at δ 3.28 and 2.61 ppm (geminal methylene protons) exhibit close spacial proximity.

Since the agreement between computation and experiment is poor in the case of conformer B (the computed values are 6.01 and 5.17 ppm, respectively), this result is again consistent with conformer A as being the true structure present in solution.

Further validation is provided by NOESY NMR experiments on cyclic phosphonamide **1b**. In conformer A, where the two naphthyl groups are constrained in a stacked structural arrangement, H_a and H_b are far away (where the distance

dx.doi.org/10.1021/jo502094g | J. Org. Chem. 2014, 79, 11101−11109

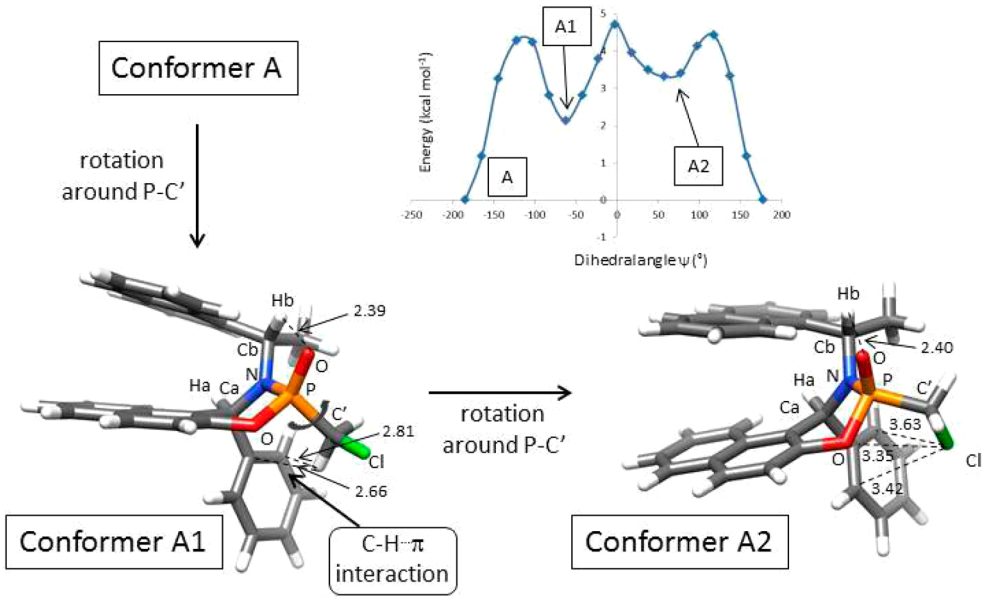

Figure 6. Conformational analysis along the dihedral angle ψ. Schematic representation of conformers A1 and A2. Energy values are expressed in kcal mol^{-1} and distances in angstroms.

estimated from the crystallographic analysis is 3.37 Å and the computed distance is 3.52 Å), while in conformers B and C these two hydrogen atoms are close together in space (i.e., the computed $H_a \cdots H_b$ distance in conformers B and C are 2.03 and 2.20 Å, respectively). As reported above, in the ^{1}H NMR spectrum of **1b**, the signals of the two methylene hydrogen atoms are centered at 3.28 and 2.61 ppm. The NOESY experiment clearly confirms that H_a and H_b are not close together (see expansion of the NOESY data in Figure 5: no cross peaks are observed between the signals at δ 5.61 and 6.15). In contrast, the experiment states the expected proximity of the two chloromethyl hydrogen atoms (interaction between the signals at 3.28 and 2.61 ppm).

4.3. Rotation of the Chloromethyl Group. The second conformational motif that was investigated is rotation of the chloromethyl group around the bond connecting phosphorus and the chloromethyl carbon atom C′. This rotation is described by the dihedral angle ψ defined by the two planes Cl−C′−P and C′−P−N (dihedral angle [Cl−(C′−P)−N]) and illustrated in Figure 6. In the same figure, we have reported the energy profile obtained in an optimized scan using angle ψ as rotational coordinate (diagram in the top right part).

The potential surface exhibits the presence of three conformational minima: previously discussed conformation A and two additional conformations A1 and A2. Conformations A and A1 are characterized by CH···π interactions between one of the two methylene hydrogen atoms and the π system of the phenyl group (see Figures 4 and 6). The strength of these interactions, which are consistent with the crystal structure, is approximately equivalent in A and A1, as suggested by the shortest distances (reported in the figures) between one methylene hydrogen and the phenyl carbon atoms (2.67 and 2.73 Å in A and 2.66 and 2.81 Å in A1). The presence in A of two interactions between the methylene hydrogen atoms and the endocyclic oxygen (CH···O distance = 2.75 and 2.81 Å) and that involving one methylene hydrogen with the exocyclic oxygen (CH···O distance = 2.98 Å) suggest that the *gauche* arrangement (torsional angle is 61.7°) of the chlorine atom with the exocyclic oxygen can be considered as a generalized anomeric effect,[38,39] which stabilizes A with respect to A1. In conformer A2, the CH···π interactions disappear and the chlorine atom is now facing the benzene π system (see Figure 5), thus increasing the energy of the system.

The structure of the most stable conformer obtained from the computational results on the isolated molecule (i.e., conformer A) does not correspond to the crystallographic structure. This structure appears to match conformer A1 of Figure 6, which is approximately 2.0 kcal mol^{-1} higher in energy than conformer A. Even if A and A1 are both characterized by a stabilizing C−H···π interaction (involving a pro-(*R*) and pro-(*S*) hydrogen of the chloromethyl moiety and the phenyl group, respectively), the solid-phase conformer A1 is favored by intermolecular interaction involving the chlorine atom of one molecule and a naphthyl C−H bond of an adjacent molecule (see the previous section and data reported in Table 1). This interaction is, however, lost in solution. Also, rotation around the P−C′ bond (in the transformation A1 → A) activates a hydrogen interaction involving the chlorine atom and one hydrogen atom of the methyl group (C−H···Cl distance = 3.00 Å, see Figure 4),[33] which further stabilizes A with respect to A1.

An energy difference of about 2.0 kcal mol^{-1} between A and A1 gives for the former structure a population of 96.7%, which indicates that in solution the molecule practically exists in a unique molecular conformation (since the low conformational barriers can be easily overcome at room temperature, this group is free to rotate and the molecule spends the major part of its time in conformation A).

The chemical shifts of the two chloromethyl hydrogen atoms computed for the most stable conformer A (3.47 and 1.80 ppm) can be considered consistent with the experimentally observed values (3.28 and 2.61 ppm respectively, as previously reported). This result enforces the hypothesis that conformer A represents the structure present in solution.

To conclude, the previously discussed stabilizing interactions involving either the two naphthyl rings or the chloromethyl group and the oxygen atoms (and, additionally, the intermolecular C−H···Cl hydrogen bond) seem to be a key-

dx.doi.org/10.1021/jo502094g | J. Org. Chem. 2014, 79, 11101−11109

factor in determining the stability of specific structures found in solid phase.

CONCLUSIONS

In the present work, we have described high stereoselective cyclization of aminobenzylnaphthols with chloromethylphosphonic dichloride, which yields almost exclusively aryl (S,S,S_P)-cyclic phosphonamides. These molecules are valuable intermediates with potential applications in asymmetric synthesis and medicinal chemistry. The X-ray diffraction analysis shows that the solid-phase structures of these intermediates are characterized by a twist-boat conformation of the C−C−C−O−P-N ring and an arrangement of the two naphthyl moieties, which represents a departure from the conformation of the starting materials to form parallel displaced stacking assemblies. This arrangement activates intramolecular stabilizing π-stacking interactions between the two aryl π systems. Analysis of the solid-state structures also suggest the existence of stabilizing CH···π interaction between one hydrogen of the chloromethyl group and a phenyl ring.

The QM computations and the NMR analysis confirm that, even in solution, the most stable structure is consistent with a parallel-displaced stacking arrangement of the two naphthyl groups, which is similar to that found in the solid state (conformer A). In contrast, the most favored conformation of the chloromethyl group present in solution does not match that of the crystallographic structure that corresponds to conformer A1. This is due to an absence in solution of specific intermolecular interactions which are present only in the solid state.

The results further indicate that the previously discussed stabilizing interactions involving either the two naphthyl rings or the chloromethyl group, and additionally, the intermolecular hydrogen bonds are responsible for the stability of specific structures found in solid phase. Also, it is reasonable to extrapolate that these stabilizing effects could have been responsible for the high stereoselection observed in this reaction.

EXPERIMENTAL SECTION

Chemicals were used as received. Elemental analyses were performed on a CHNS-O elemental analyzer. NMR spectra were recorded on a ^{1}H-500 MHz spectrometer. Only the absolute value of each coupling constant was reported. HMBC and HSQC experiments were employed for the attribution of the resonances. NOESY experiment of cyclic phosphonamide **1b** was performed on an accurately degassed sample, with a mixing time optimized for the alkyl hydrogen nuclei.

Materials. Aminobenzylnaphthols **1a−4a** were synthesized according to the previously reported methods.[18] Cyclic phosphonamides **1b−4b** were obtained from starting materials **1a−4a** with the following procedure. A solution of chloromethylphosphonic dichloride (1 mmol) and pyridine (2 mmol), in 3 mL of toluene was cooled to 0 °C. Then, a solution of aminobenzylnaphthols **1a−4a** (1.1 mmol) in 12 mL of toluene was slowly added with stirring. After 30 min of stirring, the reaction was allowed to reach room temperature and was stirred overnight. The mixture was quenched with a solution of HCl 1 N and extracted three times with ethyl acetate. The organic phase was washed with water and dried (Na_2SO_4). The crude reaction mixture was separated with column chromatography (silica gel, eluent *n*-hexane/ethyl acetate 7:3) and further purified by crystallization.

(S_P)-2-(Chloromethyl)-3-((*S*)-1-naphthalen-1-yl-ethyl)-((*S*)-4-phenyl)-3,4-dihydro-1-oxa-3-aza-2-phospha-phenanthrene 2-Oxide (1b). Isolated yield: 0.365 g (73%). Mp: 183−184 °C (from *n*-hexane/ethyl acetate 9:1). $[\alpha]^{25}_D$ = +349.1 (*c* = 0.8 in $CHCl_3$). Anal. Calcd for $C_{30}H_{25}ClNO_2P$: C, 72.36; H, 5.06; N, 2.81. Found: C, 72.16; H, 4.82; N, 3.11. ^{1}H NMR (500 MHz, $CDCl_3$): δ_H 8.19−8.12 (1H, m), 7.84−7.76 (1H, m), 7.50−7.42 (3H, m), 7.41−7.36 (1H, m), 7.32−7.24 (3H, m), 7.20−7.08 (5H, m), 6.99−6.94 (1H, m), 6.91−6.83 (2H, m), 6.44−6.39 (1H, m), 6.20−6.11 (1H, m), 5.61 (1H, d, *J* = 25.6 Hz), 3.28 (1H, dd, *J* = 11.6 Hz, *J* = 13.6 Hz), 2.61 (1H, dd, *J* = 8.9 Hz, *J* = 13.6 Hz), 2.20 (3H, d, *J* = 6.9 Hz). ^{13}C NMR (125 MHz, $CDCl_3$): δ_C 147.4 (d, *J* = 9.7 Hz), 138.8, 133.9 (d, *J* = 3.5 Hz), 133.2, 131.4, 129.7, 129.6, 129.4, 129.3 (d, *J* = 1.4 Hz), 128.8, 128.2, 127.8, 127.7, 127.1, 126.4, 125.7, 125.6, 125.2, 124.4, 124.2, 124.1 (d, *J* = 8.8 Hz), 123.1, 121.3, 118.7 (d, *J* = 4.2 Hz), 53.7 (d, *J* = 2.1 Hz), 51.8 (d, *J* = 4.2 Hz), 36.8 (d, *J* = 154.7 Hz), 22.1 (d, *J* = 2.1 Hz). ^{31}P NMR (202 MHz, $CDCl_3$): δ_P 23.5.

(S_P)-2-(Chloromethyl)-((*S*)-4-(4-fluorophenyl))-3-((*S*)-1-naphthalen-1-yl-ethyl)-3,4-dihydro-1-oxa-3-aza-2-phosphaphenanthrene 2-Oxide (2b). Isolated yield: 0.47 g (91%). Mp: 191−193 °C (from *n*-hexane/acetone 1:1). $[\alpha]^{25}_D$ = +322.9 (*c* = 0.7, $CHCl_3$). Anal. Calcd for $C_{30}H_{24}ClFNO_2P$: C, 69.84; H, 4.69; N, 2.71. Found: C, 69.61; H, 4.57; N, 3.00. ^{1}H NMR ($CDCl_3$, 500 MHz): δ_H 8.16−8.12 (1H, m), 7.81−7.76 (1H, m), 7.50−7.43 (3H, m), 7.41−7.36 (1H, m), 7.21−7.15 (1H, m), 7.14−7.07 (4H, m), 7.00−6.93 (3H, m), 6.92−6.84 (2H, m), 6.41−6.36 (1H, m), 6.14 (1H, dq, *J* = 9.5 Hz, *J* = 6.9 Hz), 5.57 (1H, d, *J* = 25.5 Hz), 3.32 (1H, dd, *J* = 11.7 Hz, *J* = 13.6 Hz), 2.63 (1H, dd, *J* = 8.9 Hz, *J* = 13.6 Hz), 2.18 (3H, d, *J* = 6.9 Hz). ^{13}C NMR ($CDCl_3$, 125 MHz): δ_C 162.4 (d, *J* = 248 Hz), 147.3 (d, *J* = 9.0 Hz), 134.7 (d, *J* = 3.5 Hz), 133.7 (d, *J* = 2.8 Hz), 133.2, 131.3, 129.7, 129.6, 129.5 (d, *J* = 7.6 Hz), 129.4, 129.1 (d, *J* = 1.4 Hz), 127.8, 127.1, 126.6, 125.7, 125.6, 125.3, 124.5, 124.2, 123.9 (d, *J* = 9.0 Hz), 123.0, 121.1, 118.7 (d, *J* = 4.2 Hz), 115.7 (d, *J* = 21.5 Hz), 53.1 (d, *J* = 2.8 Hz), 51.9 (d, *J* = 4.2 Hz), 36.8 (d, *J* = 154.7 Hz), 22.1 (d, *J* = 2.8 Hz). ^{31}P NMR (202 MHz, $CDCl_3$): δ_P 23.2.

(S_P)-2-(Chloromethyl)-((*S*)-4-(4-chlorophenyl))-3-((*S*)-1-naphthalen-1-ylethyl)-3,4-dihydro-1-oxa-3-aza-2-phosphaphenanthrene 2-Oxide (3b). Isolated yield: 0.405 g (76%). Mp: 215−216 °C (from *n*-hexane/ethyl acetate 1:1). $[\alpha]^{25}_D$ = +332.5 (*c* = 0.7, $CHCl_3$). Anal. Calcd for $C_{30}H_{24}Cl_2NO_2P$: C, 67.68; H, 4.54; N, 2.63. Found: C, 67.77; H, 4.42; N, 2.93. ^{1}H NMR (500 MHz, $CDCl_3$): δ_H 8.15−8.11 (1H, m), 7.80−7.76 (1H, m), 7.50−7.43 (3H, m), 7.41−7.36 (1H, m), 7.28−7.21 (2H, m), 7.20−7.16 (1H, m), 7.14−7.04 (4H, m), 6.99−6.95 (1H, m), 6.90−6.83 (2H, m), 6.39−6.35 (1H, m), 6.17−6.11 (1H, m), 5.56 (1H, d, *J* = 25.4 Hz), 3.34 (1H, dd, *J* = 11.6 Hz, *J* = 13.6 Hz), 2.68 (1H, dd, *J* = 8.6 Hz, *J* = 13.6 Hz), 2.18 (3H d, *J* = 6.8 Hz). ^{13}C NMR ($CDCl_3$, 125 MHz): δ_C 147.3 (d, *J* = 9.0 Hz), 137.6, 134.2, 133.7 (d, *J* = 3.5 Hz), 133.3, 131.4, 129.8, 129.7, 129.3, 129.2 (d, *J* = 1.4 Hz), 129.1, 129.0, 127.9, 127.2, 126.6, 125.8, 125.6, 125.3, 124.6, 124.3, 123.7 (d, *J* = 9.0 Hz), 123.1, 121.0, 118.7 (d, *J* = 4.6 Hz), 53.2 (d, *J* = 2.1 Hz), 52.0 (d, *J* = 4.2 Hz), 36.9 (d, *J* = 155.4 Hz), 22.1 (d, *J* = 2.8 Hz). ^{31}P NMR (202 MHz, $CDCl_3$): δ_P 22.8.

A small sample of (*S*,*S*,R_P)-**3b** has an $[\alpha]^{25}_D$ = +187 (*c* = 0.06, $CHCl_3$). ^{31}P NMR (202 MHz, $CDCl_3$): δ_P 18.0.

(S_P)-2-(Chloromethyl)-((*S*)-4-(4-bromophenyl))-3-((*S*)-1-naphthalen-1-yl-ethyl)-3,4-dihydro-1-oxa-3-aza-2-phosphaphenanthrene 2-Oxide (4b). Isolated yield: 0.29 g (50)%. Mp: 209−211 °C (from *n*-hexane/ethyl acetate 2:1). $[\alpha]^{25}_D$ = +308.7 (*c* = 1.0, $CHCl_3$). Anal. Calcd for $C_{30}H_{24}BrClNO_2P$: C, 62.46; H, 4.19; N, 2.43. Found: C, 62.57; H, 4.29; N, 2.23. ^{1}H NMR (500 MHz, $CDCl_3$): δ_H 8.14−8.11 (1H, m), 7.80−7.76 (1H, m), 7.50−7.44 (3H, m), 7.42−7.37 (3H, m), 7.21−7.16 (1H, m), 7.14−7.09 (2H, m), 7.02−6.95 (3H, m), 6.91−6.84 (2H, m), 6.38−6.35 (1H, m), 6.17−6.11 (1H, m), 5.53 (1H, d, *J* = 25.6 Hz), 3.34 (1H, dd, *J* = 11.6 Hz, *J* = 13.6 Hz), 2.69 (1H, dd, *J* = 8.8 Hz, *J* = 13.6 Hz), 2.17 (3H d, *J* = 6.9 Hz). ^{13}C NMR ($CDCl_3$, 125 MHz): δ_C 147.3 (d, *J* = 9.7 Hz), 138.2, 133.7 (d, *J* = 2.8 Hz), 133.3, 132.0, 131.4, 129.8, 129.7, 129.4, 129.2 (m), 127.9, 127.2, 126.7, 125.8, 125.7, 125.3, 124.6, 124.3, 123.7 (d, *J* = 8.3 Hz), 123.1, 122.3, 121.0, 118.8 (d, *J* = 4.9 Hz), 53.3 (d, *J* = 2.1 Hz,), 52.0 (d, *J* = 4.2 Hz), 36.9 (d, *J* = 155.4 Hz), 22.1 (d, *J* = 2.8 Hz). ^{31}P NMR (202 MHz, $CDCl_3$): δ_P 22.8.

A small sample of (*S*, *S*, R_P)-**4b** has an $[\alpha]^{25}_D$ = +108 (*c* = 0.45, $CHCl_3$). ^{31}P NMR (202 MHz, $CDCl_3$): δ_P 18.0.

X-ray Experiments. X-ray data were collected at 293 K by means of a single-crystal X-ray diffractometer with Mo Kα radiation (λ =

dx.doi.org/10.1021/jo502094g | J. Org. Chem. 2014, 79, 11101−11109

0.71073 Å); data collection: COLLECT;[40] cell refinement and data reduction: EvalCCD.[41] Data were corrected for Lorentz and polarization effects and for absorption effects.[42] Unit cell parameters are reported in Table S1 (Supporting Information). The structures were solved by the direct method procedure of SIR97[43] and refined by a full-matrix-least-squares technique based on F^2 (SHELXL-97).[44] In the refinement of the crystal structures, the hydrogen atoms were placed in idealized positions riding on their attached atoms ($C-H_{Ar}$ 0.93 Å, $C-H_{methyl}$ 0.96 Å, $C-H_{Alk}$ = 0.98 Å, $U_{iso}(H) = 1.2U_{iso}(C)$). The non-hydrogen atoms were refined with anisotropic thermal parameters. Data collection and refinement are likewise reported in Table S1 (Supporting Information). The molecules are depicted in Figures S1–S4 (Supporting Information). Complete crystallographic data are available upon request from the Cambridge Crystallographic Data Centre (12 Union Road, Cambridge, CB2 1EZ, UK; e-mail: deposit@ccdc.cam.ac.uk), or by quoting the depository numbers CCDC-1013329 (**1b**), 1013323 (**2b**), 1013325 (**3b**), and 1013324 (**4b**).

Computational Methods. All DFT computations reported were performed with the Gaussian 09 series of programs[45] using the M06-2X functional[46] and the 6-311++G** basis set.[47] The geometries of the various critical points on the potential surface were fully optimized with the gradient method available in Gaussian 09, and harmonic vibrational frequencies were computed to evaluate the nature of all critical points. Since NMR experiments were carried out in deuterated chloroform, the solvent effects was taken into account during optimization using the polarizable continuum model (PCM) using the integral equation formalism variant (IEFPCM).[48] A values of 4.71 was employed for the dielectric constant ε. NMR shielding tensors were computed with the gauge-independent atomic orbital (GIAO) method.[49]

■ ASSOCIATED CONTENT

Supporting Information

Crystallographic data and ORTEP plots of cyclic phosphonamides **1b**–**4b**. Graphical representation and geometrical parameters of the CH···π interaction in compound **1b**. Graphical representation of the ^{1}H and ^{13}C NMR spectra of cyclic phosphonamides **1b**–**4b**. This material is available free of charge via the Internet at http://pubs.acs.org

■ AUTHOR INFORMATION

Corresponding Author

*E-mail: cardellicchio@ba.iccom.cnr.it.

Notes

The authors declare no competing financial interest.

■ ACKNOWLEDGMENTS

We thank Mr. Giuseppe Chita (CNR, Istituto di Crystallografia, Bari, Italy) for the X-ray data collection and Dr. Angel Alvarez-Larena (Universitat Autònoma de Barcelona, Spain) for helpful discussions on the single-crystal X-ray structures. Thanks are due to CINMPIS consortium and to "Phoebus" Project "Tecnologie plastiche per la realizzazione di celle solari e sorgenti organiche per illuminazione ad elevata efficienza, uniformità e brillanza" in the framework of the Reti di Laboratori Pubblici di Ricerca.

■ REFERENCES

(1) Denmark, S. E.; Dorow, R. L. *J. Org. Chem.* **1990**, *55*, 5926–5928.
(2) Denmark, S. E.; Kim, J.-H. *J. Org. Chem.* **1995**, *60*, 7535–7547.
(3) Denmark, S. E.; Marlin, J. E.; Rajendra, G. *J. Org. Chem.* **2013**, *78*, 66–82 and references therein.
(4) Patani, G. A.; LaVoie, E. J. *Chem. Rev.* **1996**, *96*, 3147–3176.
(5) Grembecka, J.; Mucha, A.; Cierpicki, T.; Kafarski, P. *J. Med. Chem.* **2003**, *46*, 2641–2655.
(6) Mucha, A.; Kafarski, P.; Berlicki, Ł. *J. Med. Chem.* **2011**, *54*, 5955–5980.
(7) Lu, P.; Liu, J.; Wang, Y.; Chen, X.; Yang, Y.; Ji, R. *Biorg. Med. Chem. Lett.* **2009**, *19*, 6918–6921.
(8) Brock, N. *Cancer Res.* **1989**, *49*, 1–7.
(9) Gholivand, K.; Ghaziani, F.; Shariatinia, Z.; Dorosti, N.; Mirshahi, M.; Sarikhani, S. *Med. Chem. Res.* **2012**, *21*, 2185–2195.
(10) Sørensen, M. D.; Blæhr, L. K. A.; Christensen, M. K.; Høyer, T.; Latini, S.; Hjarnaa, P.-J. V.; Björkling, F. *Biorg. Med. Chem.* **2003**, *11*, 5461–5484.
(11) Quintero, L.; Sanchez-Vazquez, M.; Cruz-Gregorio, S.; Sartillo-Piscil, F. *J. Org. Chem.* **2010**, *75*, 5852–5859.
(12) Pietrusiewicz, K. M.; Zablocka, M. *Chem. Rev.* **1994**, *94*, 1375–1411.
(13) Cardellicchio, C.; Fiandanese, V.; Naso, F.; Pacifico, S.; Koprowski, M.; Pietrusiewicz, K. M. *Tetrahedron Lett.* **1994**, *35*, 6343–6346.
(14) Cardellicchio, C.; Naso, F.; Capozzi, M. A. M. *Tetrahedron: Asymmetry* **2004**, *15*, 1471–1476.
(15) Cardellicchio, C.; Ciccarella, G.; Naso, F.; Schingaro, E.; Scordari, F. *Tetrahedron: Asymmetry* **1998**, *9*, 3667–3675.
(16) Cardellicchio, C.; Ciccarella, G.; Naso, F.; Perna, F.; Tortorella, P. *Tetrahedron* **1999**, *55*, 14685–14692.
(17) Cardellicchio, C.; Capozzi, M. A. M.; Naso, F. *Tetrahedron: Asymmetry* **2010**, *21*, 507–517.
(18) Cardellicchio, C.; Capozzi, M. A. M.; Alvarez-Larena, A.; Piniella, J. F.; Capitelli, F. *CrystEngComm* **2012**, *14*, 3972–3981.
(19) Cimarelli, C.; Mazzanti, A.; Palmieri, G.; Volpini, E. *J. Org. Chem.* **2001**, *66*, 4759–4765.
(20) Giovenzana, G. B.; Pagliarin, R.; Palmisano, G.; Pilati, T.; Sisti, M. *Tetrahedron: Asymmetry* **1999**, *10*, 4277–4280.
(21) Hanessian, S.; Bennani, Y. L.; Delorme, D. *Tetrahedron Lett.* **1990**, *31*, 6461–6464.
(22) Bennani, Y. L.; Hanessian, S. *Tetrahedron* **1996**, *52*, 13837–13866.
(23) Lopez, B.; Maestro, A.; Pedrosa, R. *Eur. J. Org. Chem.* **2007**, 3012–3022.
(24) Surendra Babu, V. H. H.; Krishnaiah, M.; Anil Kumar, M.; Suresh Reddy, C.; Kant, R. *Acta Crystallogr.* **2009**, *E65*, o2696–o2697.
(25) Selladurai, S.; Subramanian, K.; Palanichamy, M. *Acta Crystallogr.* **1991**, *C47*, 1056–1058.
(26) Nishio, M. *CrystEngComm* **2004**, *6*, 130–158.
(27) Nishio, M. *Phys. Chem. Chem. Phys.* **2011**, *13*, 13873–13900.
(28) Nishio, M.; Umezawa, Y.; Fantini, J.; Weiss, M. S.; Chakraborti, P. *Phys. Chem. Chem. Phys.* **2014**, *16*, 12648–12683.
(29) Naso, F.; Capozzi, M. A. M.; Bottoni, A.; Calvaresi, M.; Bertolasi, V.; Capitelli, F.; Cardellicchio, C. *Chem.—Eur. J.* **2009**, *15*, 13417–13426.
(30) Capozzi, M. A. M.; Centrone, C.; Fracchiolla, G.; Naso, F.; Cardellicchio, C. *Eur. J. Org. Chem.* **2011**, 4327–4334.
(31) Capozzi, M. A. M.; Capitelli, F.; Bottoni, A.; Calvaresi, M.; Cardellicchio, C. *ChemCatChem* **2013**, *5*, 210–219.
(32) Desiraju, G. R. *J. Am. Chem. Soc.* **2013**, *135*, 9952–9967.
(33) Brammer, L.; Bruton, E. A.; Sherwood, P. *Cryst. Growth Des.* **2001**, *1*, 277–290.
(34) Metrangolo, P.; Resnati, G. *Cryst. Growth Des.* **2012**, *12*, 5835–5838.
(35) Swierczynski, D.; Luboradzki, R.; Dolgonos, G.; Lipkowski, J.; Schneider, H.-J. *Eur. J. Org. Chem.* **2005**, 1172–1177.
(36) Janowski, T.; Pulay, P. *J. Am. Chem. Soc.* **2012**, *134*, 17520–17525.
(37) Bentrude, W. G.; Setzer, W. N. Stereospecificity in ^{31}P-element Couplings: Proton-Phosphorus couplings. In *Phosphorus-31 NMR Spectroscopy in Stereochemical analysis. Organic Compounds and Metal Complexes*; Verkade, J. G., Quin, L. D., Eds.; VCH Publishers: Deerfield Beach, 1987.
(38) Wang, C.; Chen, Z.; Wu, W.; Mo, Y. *Chem.—Eur. J.* **2013**, *19*, 1436–1444.

(39) Ferro-Costas, D.; Vila, A.; Mosquera, R. A. *J. Phys. Chem. A* **2013**, *117*, 1641−1650.
(40) *Nonius: COLLECT*; Nonius B.V., Delft, The Netherlands, 1998.
(41) Duisenberg, A. J. M.; Kroon-Batenburg, L. M. J.; Schreurs, A. M. M. *J. Appl. Crystallogr.* **2003**, *36*, 220−229.
(42) Sheldrick, G. M. *SADABS, Absorption Correction Program*; University of Göttingen: Göttingen, 1996.
(43) Altomare, A.; Burla, M. C.; Camalli, M.; Cascarano, G. L.; Giacovazzo, C.; Guagliardi, A.; Moliterni, A. G.; Polidori, G.; Spagna, R. *J. Appl. Crystallogr.* **1999**, *32*, 115−119.
(44) Sheldrick, G. M. *SHELXL-97. Program for the Refinement of Crystal Structures*. University of Göttingen: Göttingen, 1997.
(45) Gaussian 09, Revision A.02: Frisch, M. J.; Trucks, G. W.; Schlegel, H. B.; Scuseria, G. E.; Robb, M. A.; Cheeseman, J. R.; Scalmani, G.; Barone, V.; Mennucci, B.; Petersson, G. A.; Nakatsuji, H.; Caricato, M.; Li, X.; Hratchian, H. P.; Izmaylov, A. F.; Bloino, J.; Zheng, G.; Sonnenberg, J. L.; Hada, M.; Ehara, M.; Toyota, K.; Fukuda, R.; Hasegawa, J.; Ishida, M.; Nakajima, T.; Honda, Y.; Kitao, O.; Nakai, H.; Vreven, T.; Montgomery, J. A., Jr.; Peralta, J. E.; Ogliaro, F.; Bearpark, M.; Heyd, J. J.; Brothers, E.; Kudin, K. N.; Staroverov, V. N.; Kobayashi, R.; Normand, J.; Raghavachari, K.; Rendell, A.; Burant, J. C.; Iyengar, S. S.; Tomasi, J.; Cossi, M.; Rega, N.; Millam, M. J.; Klene, M.; Knox, J. E.; Cross, J. B.; Bakken, V.; Adamo, C.; Jaramillo, J.; Gomperts, R.; Stratmann, R. E.; Yazyev, O.; Austin, A. J.; Cammi, R.; Pomelli, C.; Ochterski, J. W.; Martin, R. L.; Morokuma, K.; Zakrzewski, V. G.; Voth, G. A.; Salvador, P.; Dannenberg, J. J.; Dapprich, S.; Daniels, A. D.; Farkas, Ö.; Foresman, J. B.; Ortiz, J. V.; Cioslowski, J.; Fox, D. J. Gaussian, Inc., Wallingford, CT, 2009.
(46) Zhao, Y.; Truhlar, D. G. *Theor. Chem. Acc.* **2008**, *120*, 215−241.
(47) Frisch, M. J.; Pople, J. A.; Binkley, J. S. *J. Chem. Phys.* **1984**, *80*, 3265−3269.
(48) Tomasi, J.; Mennucci, B.; Cammi, R. *Chem. Rev.* **2005**, *105*, 2999−3093.
(49) Wolinski, K.; Hilton, J. F.; Pulay, P. *J. Am. Chem. Soc.* **1990**, *112*, 8251−8260.